


Preparation of Liposomal Raloxifene-Graphene Nanosheet and Evaluation of Its *In Vitro* Anticancer Effects

Dose-Response:
An International Journal
January-March 2022:1-10
© The Author(s) 2022
Article reuse guidelines:
sagepub.com/journals-permissions
DOI: 10.1177/115593258211063983
journals.sagepub.com/home/dos


Ahmed E. Altyar¹  and Omar Fahmy²

Abstract

Background: In current years, researchers have shown their prime interest in developing multifunctional drug delivery systems, especially against cancers, for effective anticancer outcomes.

Methodology: Raloxifene (RLX) loaded liposomal-graphene nanosheet (GNS) was developed. The novelty of this work was to enhance the solubilization of RLX and improvement of its bioavailability in the disease area. So, the selection of optimized formula design of experiment was implemented which produced the desired formula with the particle size of 156.333 nm. Further, encapsulation efficiency, *in vitro* release, and thermodynamic stability of optimized formulation were evaluated. The optimized formulation exhibited prolonged release of RLX for a longer period of 24 h, which can minimize the dose-related toxicity of the drug. Furthermore, optimized formulation demonstrated remarkable thermodynamic stability in terms of phase separation, creaming, and cracking.

Results: The cytotoxicity study on the A549 cell line exhibited significant ($P < .05$) results in favor of optimized formulation than the free drug. The apoptotic activity was carried out by Annexin V staining and Caspase 3 analysis, which demonstrated remarkable promising results for optimized liposomal formulation.

Conclusion: From the findings of the study, it can be concluded that the novel optimized liposomal formulation could be pondered as a novel approach for the treatment of lung cancer.

Keywords

lung cancer, liposomes, raloxifene, cell cycle analysis, apoptosis, Caspase 3 evaluation

Background

One of the major types of malignancy, which causes more than 1.6 million deaths every year, is lung cancer.^{1,2} In the case of lung cancer, current epidemiological studies also reported that the patient survival rate is below 16%.¹ Including all risk factors responsible for lung-related decease, smoking alone causes more than 75% of deaths, in which males are more affected than females because smoking habits are much common in the male population.³ Besides smoking, environmental pollutants, occupational hazards, radon gas produced by radium, and asbestos are other serious threat factors for lung cancer. Asbestos as a carcinogen is responsible for 3% of deaths.⁴ Lung cancer possesses extremely unpredictable symptoms due to its heterogeneous nature and emerges in

different areas of the lungs. Generally, lung cancer is etiologically classified into two categories, that is, non-small cell lung cancer (NSCLC) and small cell lung cancer (SCLC), in which NSCLC is the most common. Drug resistivity and non-selective toxicity in the treatment of cancer is a solemn

¹Department of Pharmacy Practice, Faculty of Pharmacy, King Abdulaziz University, Jeddah, Saudi Arabia

²Department of Urology, University Putra Malaysia (UPM), Selangor, Malaysia

Received 20 August 2021; accepted 9 November 2021

Corresponding Author:

Ahmed E. Altyar, Department of Pharmacy Practice, Faculty of Pharmacy, King Abdulaziz University, P.O. Box 80260, Jeddah 21589, Saudi Arabia.
Email: aaltyar@kau.edu.sa



obstacle because it reduces the efficacy of anticancer drugs.⁵ Therefore, a complete understanding of the resistivity mechanism and solving it is a challenging task for current drug delivery systems. Thus, drug development desperately requires the involvement of novel drug delivery approaches.

For this purpose, a liposomal delivery system is a choice of drug delivery carrier approach, which can entrap hydrophilic and hydrophobic drugs. Other major reasons behind the wide acceptability of liposomes are biocompatibility and biodegradability in body environmental conditions. It efficiently carries drug into the cancerous cells via enhanced permeability and retention (EPR) effects.⁶ In addition, liposome is also recognized as a well stable passive tumor-targeted system. Therefore in this study, raloxifene (RLX) has been loaded into liposomes. RLX is a Food and Drug Administration (FDA) approved second-generation selective estrogen receptor modulator (SERM)⁷ used to treat lung cancerous cells. RLX kills the cancerous cells by causing apoptosis via the modulation of caspases.⁸ RLX belongs to BCS class II with low solubility and high permeability, so it only possesses 2% bioavailability. In this case, liposome increases the solubility of drug molecules due to the smallest particle size and its amphiphilic nature. Liposomes also modulate the permeability and release of drugs.⁹ Thus, liposome has been a suitable carrier system for the delivery of RLX in cancerous cells, which improves the bioavailability of the drug in cancerous cells.

Graphene is build up as hexagonal networks, which contains sp² carbon atoms, and the engaged carbon atoms are attached with the help of strong covalent bonds.¹⁰ 3D graphite is also developing from graphene.¹¹ Recently, graphene is crop up in the field of nanotechnology and is used as a new tool for cancer therapeutics.¹² GNS contains single-, bi-, or some, but not more than 10, sp² hybridized sheets of carbon atoms which occur in the form of six-membered rings. So, the unique structure of GNS provides flexible mechanical, thermal, and electrical properties and diverse applicability.¹³ Because of its unique physical, chemical, and mechanical properties, graphene oxide (GO) is an excellent candidate for new biological applications. These attributes include the following: (i) GO has a variety of oxygen-containing functional groups on its edges and basal planes, such as carbonyl, hydroxyl, carboxyl, and epoxy, for good water solubility and easy surface modification; (ii) GO is primarily composed of carbon atoms, resulting in excellent biocompatibility and non-toxicity; (iii) GO has a large delocalized-electron system, which helps in achieving an excellent formula stability¹⁴⁻¹⁶ so, GO was chosen because of had outstanding properties.

For the fabrication of an optimized RLX loaded liposomal-GNS, comprehensive trials are required. Therefore, the design of the experiment (DoE) approach has been established, and results occur in the form of statistical design and mathematical equations. In this way, this system simplifies the optimization procedure to understand the impressions of various selected factors on the result.

Thus, the present study was designed with the aim of enhancing the efficacy of the drug against cancerous lung cells via the increasing bioavailability at the diseased area. Hence, a

novel optimized RLX-loaded liposomal-GNS was developed using DoE and characterized the formulation in terms of particle size and encapsulation efficiency. Further, *in vitro* release, thermodynamic stability, cytotoxicity, and cell cycle analysis were also performed.

Methods

Materials

Raloxifene hydrochloride (RLX) was a gift from SPIMACO pharmaceuticals (Qassim, Saudi Arabia). 1,2-Dipalmitoyl-sn-glycero-3-phosphocholine (DPPC) and 1,2-distearoyl-sn-glycero-3-phosphoethanolamine-N-[methoxy(polyethylene glycol)-2000] (DSPE-PEG2000) were purchased from Avanti Polar Lipids, Inc. (Alabaster, AL). Cholesterol and MTT reagent were purchased from Sigma Aldrich (St Louis, MO).

Methods

Fabrication and Optimization of RLX-Loaded Liposomal-GNS

Experimental design for optimization of RLX-loaded liposomal-GNS. The RLX-loaded liposomal-GNS was optimized using the DoE (Table 1). The concentration of RLX (X1) and sonication time (X2) were selected as the independent variable, whereas particle size was picked as the response. The experimental design was produced and evaluated by Statgraphics software (Statgraphics Technologies, Inc., Warrenton, VA, USA).¹⁷

Preparation of liposomes. Thin-film hydration technique was used for the fabrication of RLX-loaded liposomes. For this purpose, 5 mg/mL DSPE-PEG2000, DPPC, and cholesterol were dispersed in chloroform in the molar ratio of 12:1:8. Then, a rotary evaporator (Heidolph, Schwabach, Germany) was used for the removal of organic at 50°C under high vacuum till a thin film of lipid appeared, and the developed film was incubated overnight at room temperature. Further, RLX and GNS (5 µg/mL) were passively entrapped into liposomes during the lipid film hydration. For this purpose, RLX was added to lipid film in different concentrations (Table 1) with continuous vigorous mixing at 50°C. Thereupon, final dispersion was sonicated for various durations as mentioned in Table 1 using ultrasonic probe sonicator (Sonics, USA) and then incubated overnight at 4°C. Ultimately, the liposomes were dialyzed using dialysis membrane (molecular weight cutoff 12 kDa) against phosphate buffer solution (PBS).¹⁸

Optimization of RLX-loaded liposomal-GNS. From the different experimental trials, the RLX-loaded liposomal-GNS was optimized using a numerical method.¹⁹ All runs were tripled to assess dispersion. The minimum value for the particle size (response) was identified as an aim in the DoE software for

Table 1. Independent Variables and Obtained Responses with Codes and Values for the Design of Experiments for the Optimization of RLX-Loaded Liposomal-GNS.

Run	X1		X2		Response I	
	A: RLX (μM)		B: ST (min)		Particle Size (nm) Observed	Particle Size (nm) Fitted
1	1.0		8.0		161.0	156.333
2	5.0		5.0		311.0	307.333
3	5.0		2.0		323.0	325.0
4	3.0		2.0		253.0	255.333
5	3.0		8.0		211.0	214.0
6	1.0		2.0		198.0	193.667
7	3.0		5.0		245.0	239.667
8	1.0		8.0		171.0	180.0
9	5.0		8.0		278.0	279.667
Factors			Levels			
Independent variables			Low	High		Optimum
A = RLX			1	5		1
B = ST			2	8		8
Dependent variables			Goal			
RI = Fitted particle size (nm)			156.333			

Note. RLX, Raloxifene; ST, Sonication time.

numerical optimization. The software suggested optimal equation was further arranged, characterized, and evaluated.

Particle size. The particle size of different trials liposomal formulation was determined via the dynamic light scattering (DLS) method using Zetasizer Nano ZS instrument (Malvern Instruments Ltd, Malvern, Worcestershire, UK) at 25°C. In this case, the particle size of prepared liposomes was analyzed by diluting 100-fold in deionized water.²⁰ The results were expressed as the average of 5 determinations. The parameters were the following: laser wavelength of 633 nm, scattering angle of 173, temperature of 25 C, medium viscosity of .8872 cP, and medium refractive index of 1.33.

Evaluation of the Optimized RLX-Loaded Liposomal-GNS

Encapsulation efficiency. The encapsulation efficiency of the prepared liposomal formulation was analyzed by lyzing formulation with 10% SDS (w/v). For this purpose, the liposomal suspension was centrifuged for 15 min at 13,000 r/min. Then encapsulated RLX in liposomes and GNS were quantified via UV-Visible spectrophotometer (PROM version 0.000, Shanghai Lab Spectrum Instruments Co., Ltd., China) at 287 nm and 300 nm, respectively.¹⁸ Then percentage entrapment efficiency was determined using the following equation²¹

Percentage entrapment efficiency

$$= \frac{\text{Total drug added} - \text{Unentrapped drug found}}{\text{Total drug added}} \quad (1)$$

In vitro release study. In order to determine the release profile of optimized RLX-loaded liposomal-GNS in comparison to conventional suspension, 2 mL of prepared liposomal formulation and conventional formulation were kept in the separate dialysis bag (molecular weight cutoff 12 kDa). Then tightly sealed dialysis bags were immersed in the 500 mL PBS (pH 7.4) at 37°C with gentle agitation. At a fixed time interval, 1 mL of sample was collected from the PBS medium, and the same amount of fresh PBS was added instantly. Thereafter, collected samples were quantified spectrophotometrically at 287 nm and cumulative percentage drug released was obtained.²²

Analysis of Thermodynamic Stability

In order to obtain the thermodynamic stability of the optimized RLX-loaded liposomal-GNS, a method reported by Kotta and associates in 2013 was implemented.²³ In this case, various test conditions (Table 2) were employed, such as centrifugation, heating-cooling cycle (HCC), and freeze-thaw cycle (FTC).¹⁷

Cytotoxicity

The cytotoxicity efficacy of optimized RLX-loaded liposomal-GNS was performed on the A549 cell line using MTT assay. For this experiment, selected cells were grown in 96 well plates at the density of 5×10^3 cells per well and incubated overnight. After stabilization, cells were treated with GO, RLX-Raw, and RLX-GO and incubated for 24 h. Then, previously treated cells were further treated with 5.0 mg/mL MTT solution (10 μL) and then incubated for 4 h at 37°C. Additionally, the collected supernatant was dispersed in 100 mL of DMSO to solubilize the formazan crystal. Samples were analyzed employing a

Table 2. Different Thermodynamic Stability Testing Conditions.

Name of Tests	Analytical Condition	Parameters
Centrifugation	30 min, 500 r/min	Creaming, cracking, and phase separation
Heating-cooling cycle	48 h at 4°C and 40°C for 3 cycles	
Freeze-thaw cycle	48 h at -20°C and 25°C for 3 cycles	

microplate reader at 570 nm. Studies were carried out in triplicate.²⁴

Cell Cycle Analysis

To analyze the effects of samples on the cell cycle, the flow cytometry method was utilized. The cells were treated with various sample formulations such as GO, RLX-Raw, and RLX-GO and incubated for 24 h. After completion of incubation, cells were separated by centrifugation and fixed with 70% cold ethanol. Before washing of samples with PBS, samples were again separated by centrifugation. Separated cells were further stained with PI and RNase before starting flow cytometry analysis.^{19,25}

Analysis of Apoptosis by Annexin V Staining

In order to analyze the comparative apoptotic activity of GO, RLX-Raw, and RLX-GO, the Annexin V method was implemented. For this purpose, selected cells were grown in six well plates at the density of 1×10^5 cells per well and then incubated overnight with IC₅₀ concentration of samples for 24 h at 37°C. Then all samples were centrifuged at 200g for 5 min, and collected cells were re-suspended in PBS at room temperature after dual washing. Further, 10 µL Annexin V and 5 µL propidium iodide (PI) solution supernatant were dispersed in the previously prepared samples and incubated at 25°C for 5 min. Final samples were analyzed using a flow cytometer (FACS Calibur, BD Bioscience, CA, USA) in triplicate.^{26,27} Phosphatidylserine (PS) translocation or externalization precedes the loss of membrane integrity that occurs in the final stages of cell death caused by either apoptotic or necrotic processes. As a result, Annexin V staining is often employed in conjunction with a vital dye, such as PI, to identify early and late apoptotic cells. Viable cells with intact membranes exclude PI, whereas the membranes of dead and injured cells are permeable to PI. As a result, healthy cells are both Annexin V and PI negative, whereas cells in early apoptosis are both Annexin V and PI positive.

Analysis of Caspase 3

The Caspase 3 determination was carried out through the Caspase 3 Colorimetric Assay Kit (BioVision, Milpitas, CA, USA). In this case, A549 cells were grown in the density of 3×10^6 cells per well and treated with control, GO, RLX-Raw, and RLX-GO. Then samples were re-suspended in ice-chilled lysate buffer and incubated in an ice medium for 10 min before centrifugation (10 000g for 1 min). The analysis

method for the Caspase 3 assay was carried according to the instructions of the manufacturer, and the developed color was determined by a microplate reader at 405 nm.^{17,19}

Statistical Analysis

Data of the current study are mentioned as the mean \pm standard deviation (SD) after triplicate experimentation. The significance of the study was analyzed from Analysis of variance (ANOVA) followed by Tukey's post hoc test. The *P* value < .05 represented the statistical significance of the data obtained.

Results

Fabrication and Optimization of RLX-Loaded Liposomal-GNS

Selection of optimized RLX-loaded liposomal formulation using design of experiment. RLX-loaded liposomal formulation was fabricated by using RLX and ST as independent variables, and particle size was selected as a dependent variable for optimization. The software suggested 9 formulations from selected independent variables, and these formulations were fabricated and characterized against particle size.

The variance analysis data procured for particle size is depicted in Table 3. The obtained *P* value declared the statistical significance of picked independent variables and their effects on the particle size of different liposomal formulations. In addition, the relationship between RLX and ST was also observed to be significant. Besides, in these independent variables, ST had a much significant influence over the dependent variable. The value of R-square was 99.3202%, and the adjusted *R*² was 98.1873%. Besides, the obtained and fitted data for particle size were in worthiness acceptance with each other, as shown in Table 3.

Equation (2) expressed the software suggested polynomial equation for particle size. The effects of every independent variable over the selected dependent variable (response) can be recognized by the regression coefficient of the polynomial equation. The positive sign for the regression coefficient for any variables proposed a positive effect of a particular variable on particle size and vice versa. So, the regression coefficient for RLX was +127.333, proposed the maximum quantity of RLX increased the particle size of the formulation. Whereas the negative value (-41.3333) for ST exhibited a negative effect on particle size, it means maximum ST reduced the particle size of the formulation. The impact of independent variables on particle size was hypothesized from the following equation (2)

Table 3. Analysis of Variance (ANOVA) Data for Particle Size Recorded in Various Suggested Trials During the Design of Experiments for the Liposomal Formulation.

Source	Sum of Squares	Degree of Freedom	Square of Mean	F-ratio	P value
A: RLX	24,320.7	1	24,320.7	395.10	.0003
B: ST	2562.67	1	2562.67	41.63	.0076
AA	32.0	1	32.0	.52	.5230
AB	16.0	1	16.0	.26	.6453
BB	50.0	1	50.0	.81	.4339
Total error	184.667	3	61.5556		
Total (corr.)	27,166.0	8			

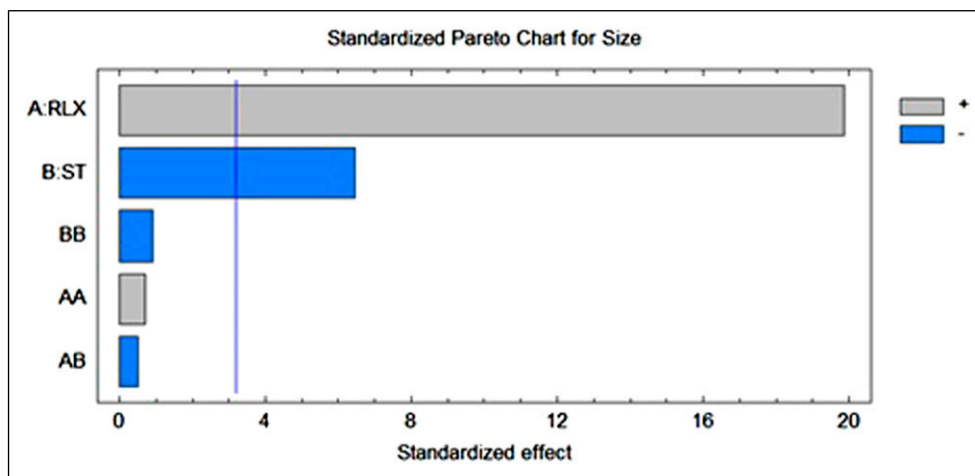


Figure 1. Pareto chart for particle size where RLX represents the concentration of raloxifene and ST represents the duration of sonication time.

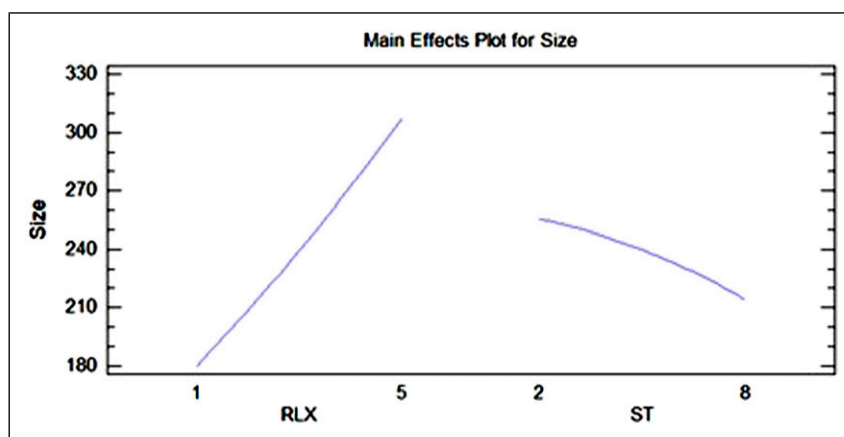


Figure 2. Main effects plot for particle size.

$$\text{Particle size} = 168.722 + 27.5 \times A - 0.333333 \times B + 1.0 \times A^2 - 0.333333 \times A \times B - 0.555556 \times B^2 \quad (2)$$

In [Figure 1](#), the Pareto chart shows the significant effects of RLX and ST and the collective effect of both independent

variables. From the outcomes, it was established that the particle size of liposomal formulations was increased with an increased quantity of RLX and decreased ST. [Figure 2](#) as the main effect plot endorsed the outcomes of the Pareto chart. [Figure 2](#) demonstrates the significant positive effect of RLX and the negative effect of ST on particle size, but in comparison to

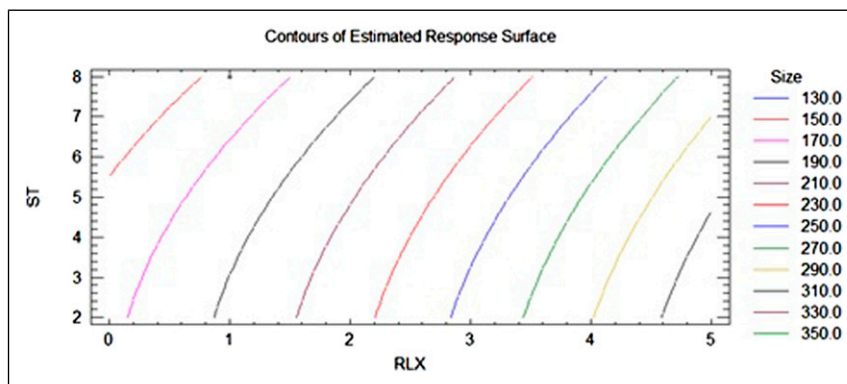


Figure 3. Contours plot for particle size.

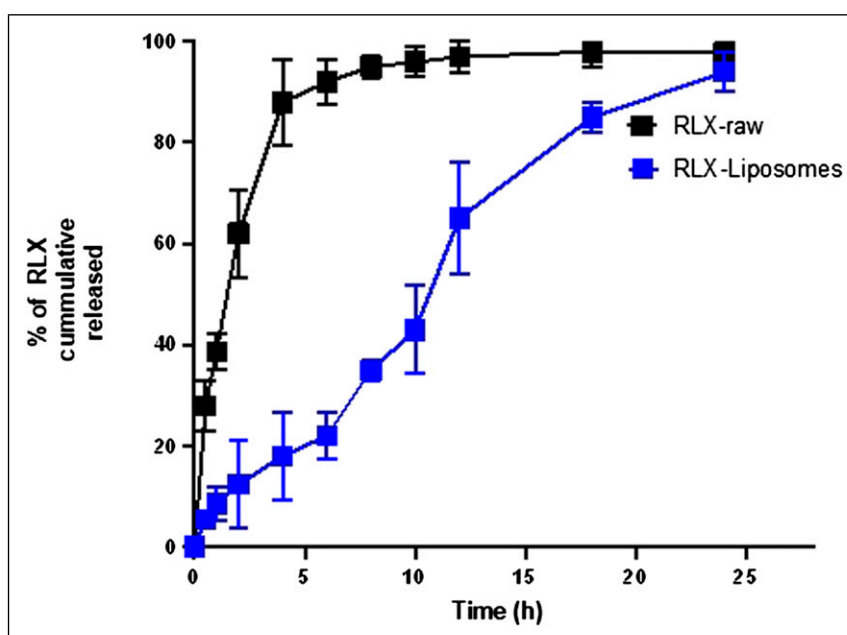


Figure 4. The *in vitro* release pattern of drug from optimized RLX-loaded liposomal-GNS and RLX-Raw.

RLX, ST exhibited a lower effect on particle size. The contours plot, as shown in Figure 3, evaluated the response surface. The contours plot also endorsed the positive impact of RLX and the negative effect of ST on the particle size of liposomal formulations. Thus, from the comprehensive statistical calculation, the optimized formula was selected.

Encapsulation Efficiency of RLX-Loaded Liposomal-GNS

The encapsulation efficiency of the RLX-loaded liposomal-GNS was analyzed, and it was found to be 54.9 ± 4.903 . In this case, RLX was encapsulated in the liposomal vesicles, and it was also due to the maximum ST. This enhanced ST reduced the particle size and provided the utmost surface area for the encapsulation RLX. The obtained result of encapsulation

efficiency also supported the previous study of liposomal-GNS formulation.¹⁸

In Vitro Release Study

The comparative *in vitro* release profile between RLX-loaded liposomal-GNS and RLX-Raw was established. Outcomes of *in vitro* release study demonstrated sustained release of RLX from the liposomal formulation. In contrast, quick fast release of RLX was observed from conventional RLX suspension in terms of percent cumulative release (Figure 4). Figure 4 demonstrated 20% cumulative release of RLX from liposomal formulation, and simultaneously 93% RLX was released from conventional suspension within 5 h. During study duration, that is, 24 h- liposomal formulation continuously released drug in a sustained manner.

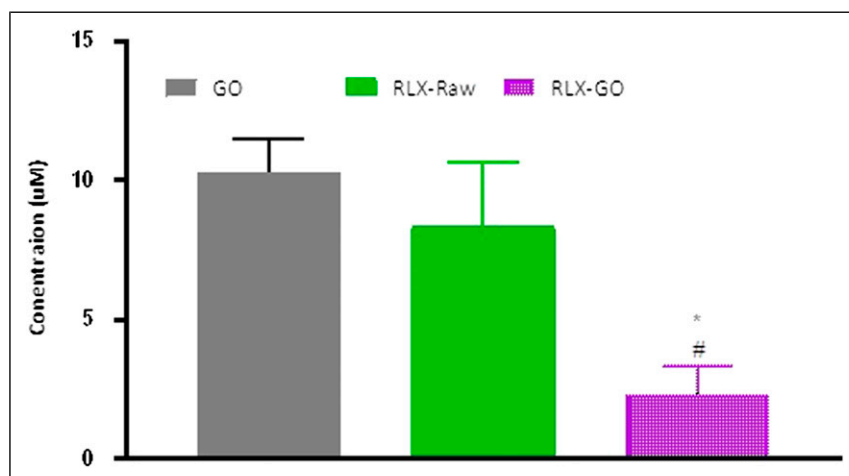


Figure 5. Comparative cytotoxicity of various samples in terms of IC₅₀. *Significantly different from graphene oxide $P < .05$, #significantly different from RLX-Raw $P < .05$. Data represent mean of ($n = 3$) independent replicates \pm SD.

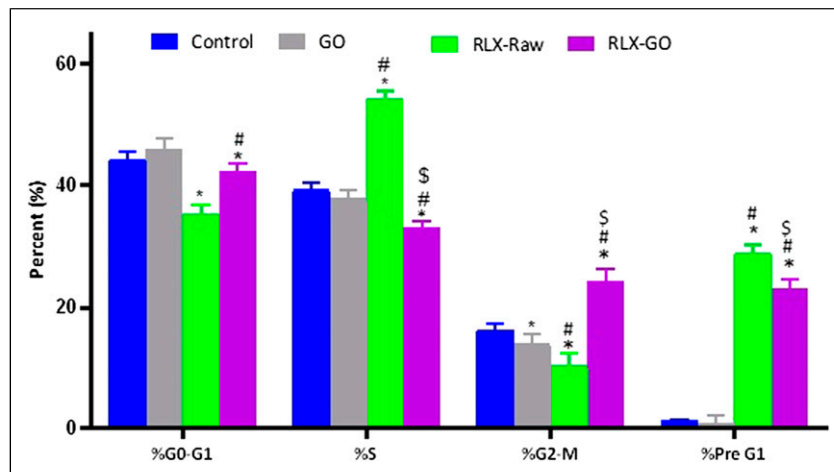


Figure 6. Effect of various formulations on cell cycle. *Significantly different from control $P < .05$, #significantly different from graphene oxide $P < .05$, \$significantly different from RLX-Raw $P < .05$.

Analysis of Thermodynamic Stability

The thermodynamic stability study results demonstrated the optimized RLX-loaded liposomal-GNS was stable in different mentioned environmental conditions. Thus, the absence of cracking, creaming, and phase separation was recorded in the optimized formulation.

Cytotoxicity Study

In order to obtain IC₅₀ of different samples, a comparative cytotoxicity study was performed, and the result is depicted in Figure 5. The novel RLX-GO formulation demonstrated the lowest IC₅₀ ($2.5 \pm 1.19 \mu\text{M}$) in comparison to GO ($10.5 \pm 2.87 \mu\text{M}$) and RLX-Raw ($8.2 \pm 2.97 \mu\text{M}$). Thus, the results indicated that when RLX was encapsulated in novel liposomal GNS, the IC₅₀ of RLX was also reduced by half. MTT assay is a colorimetric assay for measuring

cell metabolic activity. It is based on the ability of nicotinamide adenine dinucleotide phosphate (NADPH)-dependent cellular oxidoreductase enzymes to reduce the tetrazolium dye MTT to its insoluble formazan, which has a purple color

Cell cycle analysis. The effect of various formulations/samples such as control, GO, RLX-Raw, and RLX-GO on cell cycle was determined. Outcomes of the study clearly demonstrated a significantly higher percentage of cells in the G2-M phase after treatment with optimized RLX-GO formulation. Whereas, RLX-GO formulation was unable to produce significant results in G0-G1, S, and pre-G1 phase (Figure 6).

Outcomes of Annexin V staining. The apoptotic study of various samples was carried out by using flow cytometry after staining by Annexin V. Outcomes of apoptosis study demonstrated that RLX-GO formulation remarkably accelerated early, total, and

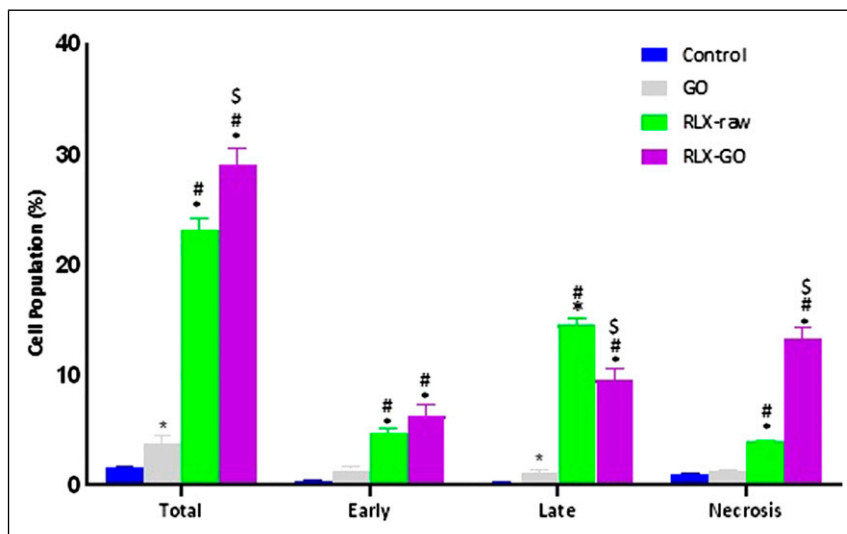


Figure 7. Determination of cellular mortality after Annexin V staining by using flow cytometry. *Significantly different from control $P < .05$, #significantly different from graphene oxide $P < .05$, \$significantly different from RLX-Raw $P < .05$. Data represent mean of ($n = 3$) independent replicates \pm SD.

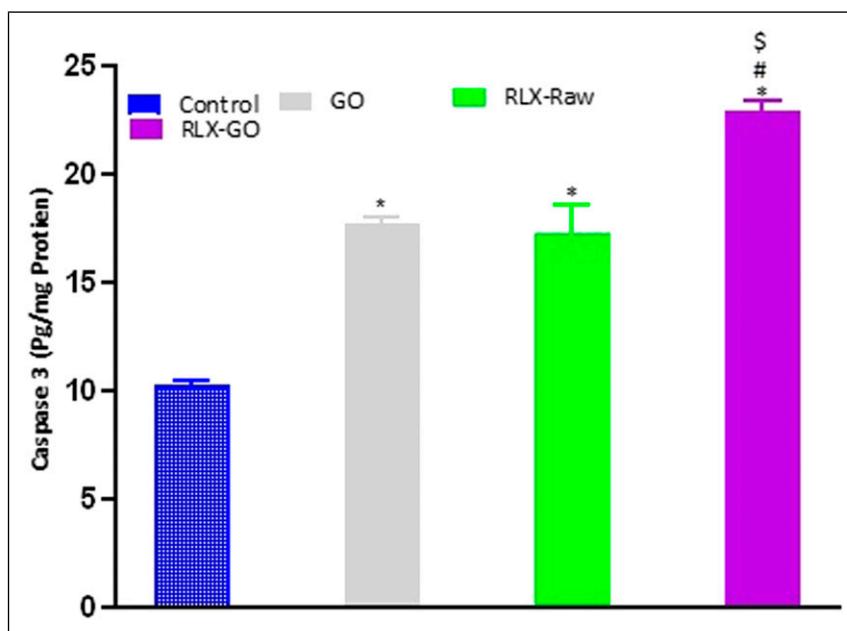


Figure 8. Comparative effects of RLX-loaded on Caspase 3. *Significantly different from control $P < .05$, #significantly different from graphene oxide $P < .05$, \$significantly different from RLX-Raw $P < .05$. Data represent mean of ($n = 3$) independent replicates \pm SD.

in necrotic cell apoptosis compared to control, GO, and RLX-Raw (Figure 7). Whereas, maximum late apoptosis was exhibited by RLX-Raw formulation.

Analysis of Caspase 3. The result of Caspase 3 analysis clearly exhibited that RLX-loaded liposomal GNS significantly increased the Caspase 3 quantity in treated cells as compared to RLX-Raw (Figure 8). Besides, GO also demonstrated an increment in the amount of Caspase 3 as compared to the control group.

Discussion

The optimized formula for the fabrication of RLX-loaded liposomal GNS was determined by DoE using Statgraphics software.¹⁷ In this model, the R^2 value of predicted and adjusted was in an acceptable relationship certifying the model validity. Independent variables such as RLX were exerting positive effects, whereas ST showed negative effects over the particle size of liposomal formulations. The optimized formula contained 1 mg RLX and 8 min required for the desired

formulation, which produced a particle size of 156.333 (fitted). Further, RLX was released from the optimized liposomal formulation at a sustained rate for a prolonged period of time, that is, 25 h. The initial slow and sustained release of RLX from optimized formulation could be due to a lessening membrane fluidity phospholipid bilayer. So, it prevents the burst release of drug from vesicles. Besides, the smallest particle size controlled the release rate and improved the dissolution rate for maximum solubilization of drug molecules. Thus, the optimized liposomal formulation is allowed to drug release for a prolonged duration in a sustained manner, and it can also minimize the dose-related toxicities.²⁸ Analysis of thermodynamic stability has endorsed the stability of optimized formulation in terms of phase separation, cracking, and creaming. The data of cytotoxicity study indicated the highest potency of optimized formulation than free drug molecules, and it occurred due to the maximum cellular permeability of liposomal formulation within cells. Besides, optimized liposomal formulation demonstrated significant maximum cell fraction in the G2-M phase indicating a progression of the cytotoxic behavior of RLX via optimized liposomal formulation. Furthermore, the higher cells proportion also indicated apoptotic behavior of optimized liposomal formulation. The observed enhancement of the anti-proliferative properties of the prepared RLX-GO formula was further substantiated by assessing its impact on cell cycle phases. DNA flow cytometric analysis showed that a significant accumulation of A549 cells in the G2-M and pre-G1 phases was caused by RLX. The tremendous apoptotic activity of optimized liposomal formulation was further testified by Annexin V staining and Caspase 3 analysis. Annexin V staining indicated results in early, total, and in necrotic cell apoptosis persuaded by optimized liposomal formulation compared to control, GO, and RLX-Raw cell death. Caspase 3 is pondered as a well-established apoptosis marker. During apoptosis, Caspase 3 acts as the last slayer Caspase, which

regulates fragmentation of DNA and annihilation of cellular proteins. Besides, the increment in the quantity of Caspase 3 is also due to the alterations in the MMP pathway which is responsible for the initiation and activation of Caspase 3. Therefore, it means RLX-GO might also cause apoptosis via modulation of MMP pathways.^{29,30} At this moment, the novel RLX-GO produced results in support of previous studies.^{31,32} These data provide additional support for augmented pro-apoptotic activities. Moreover, the observed augmentation in the cytotoxicity of RLX by loading with GO highlights a potential role for GO. Thus, the role of GO alone cannot be excluded.

Conclusion

The goal of this research was to increase bioavailability and anti-lung cancer action in the affected area. An optimal liposomal formulation was obtained by fabricating RLX-loaded liposomal GNS and optimizing it utilizing the DoE. Particle size, encapsulation efficiency, in vitro release, and thermodynamic stability were all tested for the produced liposomal formulation. As a result, the optimized RLX-loaded liposomal GNS produced a particle size of 156.333 nm with a $54.9 \pm 4.903\%$ encapsulation. Further, when compared to the free drug-contained suspension, the in vitro release analysis showed outstanding results in favor of the improved formulation. Furthermore, the cytotoxicity analysis showed that improved formulations outperformed free medication molecules. The improved formulation's remarkable apoptotic activity was further revealed by cell cycle, Annexin V, and Caspase 3 study. As a result, the bioavailability of this created innovative optimal formulation was improved, while dose-related undesirable toxicity was reduced. As a result of the findings of this investigation, the improved therapeutic efficacy of RLX in the future could be regarded a unique technique for lung cancer treatment.

Appendix

Notation

TQ Thymoquinone

Acknowledgments

The authors, therefore, acknowledge with thanks DSR for technical and financial support.

Declaration of Conflicting interests

The author(s) declared no potential conflicts of interest with respect to the research, authorship, and/or publication of this article.

Funding

The author(s) disclosed receipt of the following financial support for the research, authorship, and/or publication of this article: This Project

was funded by the Deanship of Scientific Research (DSR) at King Abdulaziz University, Jeddah, under grant no. (G-260-166-1441).

ORCID iD

Ahmed E. Altyar  <https://orcid.org/0000-0003-3747-5408>

References

1. Iqbal MA, Arora S, Prakasam G, Calin GA, Syed MA. MicroRNA in lung cancer: Role, mechanisms, pathways and therapeutic relevance. *Mol Aspects Med.* 2019;70:3-20.
2. Hung J-Y, Chang W-A, Tsai Y-M, et al. Tricetin, a dietary flavonoid, suppresses benzo(a)pyrene-induced human non-small cell lung cancer bone metastasis. *Int J Oncol.* 2015;46:1985-1993.
3. MacKinnon AC, Kopatz J, Sethi T. The molecular and cellular biology of lung cancer: Identifying novel therapeutic strategies. *Br Med Bull.* 2010;95:47-61.

4. Fatima M, Iqbal MK, Iqbal A, et al. Current insight into the therapeutic potential of phytocompounds and their nanoparticle-based systems for effective management of lung cancer [published ahead of print July 8, 2021]. *Anti Cancer Agents Med Chem*. doi: [10.2174/1871520621666210708123750](https://doi.org/10.2174/1871520621666210708123750).
5. Jin X, Yang Q, Zhang Y. Synergistic apoptotic effects of apigenin TPGS liposomes and tyroservatide: Implications for effective treatment of lung cancer. *Int J Nanomed*. 2017;12:5109-5118.
6. Zhang T, Chen Y, Ge Y, Hu Y, Li M, Jin Y. Inhalation treatment of primary lung cancer using liposomal curcumin dry powder inhalers. *Acta Pharm Sin B*. 2018;8:440-448.
7. Taurin S, Allen KM, Scandlyn MJ, Rosengren RJ. Raloxifene reduces triple-negative breast cancer tumor growth and decreases EGFR expression. *Int J Oncol*. 2013;43:785-792.
8. Almutairi FM, Abd-Rabou AA, Mohamed MS. Raloxifene-encapsulated hyaluronic acid-decorated chitosan nanoparticles selectively induce apoptosis in lung cancer cells. *Bioorg Med Chem*. 2019;27:1629-1638.
9. Patil PH, Belgamwar VS, Patil PR, Surana SJ. Solubility enhancement of raloxifene using inclusion complexes and cogrinding method. *J Pharm (Lahore)*. 2013;2013:1-9.
10. Malard LM, Pimenta MA, Dresselhaus G, Dresselhaus MS. Raman spectroscopy in graphene. *Phys Rep*. 2009;473:51-87.
11. Rao CNR, Sood AK, Subrahmanyam KS, Govindaraj A. Graphene: The new two-dimensional nanomaterial. *Angew Chem Int Ed Engl*. 2009;48:7752-7777.
12. Gao Y, Zou X, Zhao JX, Li Y, Su X. Graphene oxide-based magnetic fluorescent hybrids for drug delivery and cellular imaging. *Colloids Surf B Biointerfaces*. 2013;112:128-133.
13. Thomas D-G, Kavak E, Hashemi N, Montazami R, Hashemi N. Synthesis of graphene nanosheets through spontaneous sodiation process. *C J Carbon Res*. 2018;4:42.
14. Lin J, Chen X, Huang P. Graphene-based nanomaterials for bioimaging. *Adv Drug Deliv Rev*. 2016;105:242-254.
15. Geim AK. Graphene: Status and prospects. *Science*. 2009;324:1530-1534.
16. Nakanishi W, Minami K, Shrestha LK, Ji Q, Hill JP, Ariga K. Bioactive nanocarbon assemblies: Nanoarchitectonics and applications. *Nano Today*. 2014;9:378-394.
17. Md S, Alhakamy NA, Aldawsari HM, et al. Formulation design, statistical optimization, and in vitro evaluation of a naringenin nanoemulsion to enhance apoptotic activity in a549 lung cancer cells. *Pharmaceutics (Basel)*. 2020;13:1-21.
18. Tajvar S, Mohammadi S, Askari A, et al. Preparation of liposomal doxorubicin-graphene nanosheet and evaluation of its in vitro anti-cancer effects. *J Liposome Res*. 2019;29:163-170.
19. Alhakamy NA, A Fahmy U, Badr-Eldin SM, et al. Optimized icariin phytosomes exhibit enhanced cytotoxicity and apoptosis-inducing activities in ovarian cancer cells. *Pharmaceutics*. 2020;12:346.
20. Alhakamy NA, Ahmed OAA, Fahmy UA, Md S. Development and in vitro evaluation of 2-methoxyestradiol loaded polymeric micelles for enhancing anticancer activities in prostate cancer. *Polymers (Basel)*. 2021;13:884.
21. Iqbal MK, Iqbal A, Imtiyaz K, et al. Combinatorial lipid-nanosystem for dermal delivery of 5-fluorouracil and resveratrol against skin cancer: Delineation of improved dermatokinetics and epidermal drug deposition enhancement analysis. *Eur J Pharm Biopharm*. 2021;163:223-239.
22. Jain AS, Goel PN, Shah SM, et al. Tamoxifen guided liposomes for targeting encapsulated anticancer agent to estrogen receptor positive breast cancer cells: In vitro and in vivo evaluation. *Biomed Pharmacother*. 2014;68:429-438.
23. Kotta S, Khan AW, Ansari SH, Sharma RK, Ali J. Formulation of nanoemulsion: A comparison between phase inversion composition method and high-pressure homogenization method. *Drug Deliv*. 2015;22:455-466.
24. Ağardan NBM, Değim Z, Yılmaz Ş, Altıntaş L, Topal T. The effectiveness of raloxifene-loaded liposomes and cochleates in breast cancer therapy. *AAPS PharmSciTech*. 2016;17:968-977.
25. Hu G, Cun X, Ruan S, et al. Utilizing G2/M retention effect to enhance tumor accumulation of active targeting nanoparticles. *Sci Rep*. 2016;6:27669.
26. Faramarzi L, Dadashpour M, Sadeghzadeh H, Mahdavi M, Zarghami N. Enhanced anti-proliferative and pro-apoptotic effects of metformin encapsulated PLGA-PEG nanoparticles on SKOV3 human ovarian carcinoma cells. *Artif Cells Nanomed Biotechnol*. 2019;47:737-746.
27. Alhakamy NA, Shadab M. Repurposing itraconazole loaded PLGA nanoparticles for improved antitumor efficacy in non-small cell lung cancers. *Pharmaceutics*. 2019;11:685.
28. Layek B, Mukherjee B. Tamoxifen citrate encapsulated sustained release liposomes: Preparation and evaluation of physicochemical properties. *Sci Pharm*. 2010;78:507-515.
29. Anwar MM, Abd El-Karim SS, Mahmoud AH, Amr AE-GE, Al-Omar MA. A comparative study of the anticancer activity and PARP-1 inhibiting effect of benzofuran-pyrazole scaffold and its nano-sized particles in human breast cancer cells. *Molecules*. 2019;24:2413.
30. Ghorab MM, Alsaid MS, Samir N, et al. Aromatase inhibitors and apoptotic inducers: Design, synthesis, anticancer activity and molecular modeling studies of novel phenothiazine derivatives carrying sulfonamide moiety as hybrid molecules. *Eur J Med Chem*. 2017;134:304-315.
31. Yassemi A, Kashanian S, Zhaleh H. Folic acid receptor-targeted solid lipid nanoparticles to enhance cytotoxicity of letrozole through induction of caspase-3 dependent-apoptosis for breast cancer treatment. *Pharm Dev Technol*. 2020;25:397-407.
32. Kim CG, Castro-Aceituno V, Abbai R, et al. Caspase-3/MAPK pathways as main regulators of the apoptotic effect of the phyto-mediated synthesized silver nanoparticle from dried stem of *Eleutherococcus senticosus* in human cancer cells. *Biomed Pharmacother*. 2018;99:128-133.